IEEE Access
Multidisciplinary ⋮ Rapid Review ⋮ Open Access Journal

Received July 21, 2020, accepted August 29, 2020, date of publication September 8, 2020, date of current version September 24, 2020.

Digital Object Identifier 10.1109/ACCESS.2020.3022829

Predictive Modeling of Antibiotic Susceptibility in *E. Coli* Strains Using the U-Net Network and One-Class Classification

NAIRVEEN ALI[1,2], JOHANNA KIRCHHOFF[1,2,3,4], PATRICK IGOCHE ONOJA[1,2], ASTRID TANNERT[2,3], UTE NEUGEBAUER[1,2,3,4], JÜRGEN POPP [1,2,3,4], AND THOMAS BOCKLITZ[1,2]

[1]Institute of Physical Chemistry (IPC), Friedrich Schiller University Jena, 07743 Jena, Germany
[2]Leibniz Institute of Photonic Technology (Leibniz-IPHT), 07745 Jena, Germany
[3]Center for Sepsis Control and Care (CSCC), Jena University Hospital, 07747 Jena, Germany
[4]InfectoGnostics Forschungscampus Jena, 07743 Jena, Germany

Corresponding author: Thomas Bocklitz (thomas.bocklitz@uni-jena.de)

This work was supported in part by the Bundesministerium für Bildung und Forschung through the Project Uro-MDD and the Center for Sepsis Control and Care (CSCC, Integrated Research and Treatment Center) under Grant FKZ 03ZZ0444J and Grant FKZ 01EO1502, in part by the Deutsche Forschungsgemeinschaft through the Core Facility Jena Biophotonic and Imaging Laboratory (JBIL) under Project BO4700/4-1, in part by the InfectoGnostics Research Campus under Grant FKZ 13GW0096F, in part by the Leibniz ScienceCampus InfectoOptics which was financed by the funding line Strategic Networking of the Leibniz Association, in part by the Ministry for Economics, Sciences and Digital Society of Thuringia (TMWWDG) through the framework of the Landesprogramm ProDigital under Grant DigLeben-5575/10-9, and in part by the Free State of Thuringia which was co-financed by the European Union funds within the framework of the European Social Fund (ESF) under Grant 2019 FGR 0083. The publication of this article was funded by the Open Access Fund of the Leibniz Association.

ABSTRACT The antibiotic resistance of bacterial pathogens has become one of the most serious global health issues due to misusing and overusing of antibiotics. Recently, different technologies were developed to determine bacteria susceptibility towards antibiotics; however, each of these technologies has its advantages and limitations in clinical applications. In this contribution, we aim to assess and automate the detection of bacterial susceptibilities towards three antibiotics; *i.e.* ciprofloxacin, cefotaxime and piperacillin using a combination of image processing and machine learning algorithms. Therein, microscopic images were collected from different *E. coli* strains, then the convolutional neural network U-Net was implemented to segment the areas showing bacteria. Subsequently, the encoder part of the trained U-Net was utilized as a feature extractor, and the U-Net bottleneck features were utilized to predict the antibiotic susceptibility of *E. coli* strains using a one-class support vector machine (OCSVM). This one-class model was always trained on images of untreated controls of each bacterial strain while the image labels of treated bacteria were predicted as control or non-control images. If an image of treated bacteria is predicted as control, we assume that these bacteria resist this antibiotic. In contrast, the sensitive bacteria show different morphology of the control bacteria; therefore, images collected from these treated bacteria are expected to be classified as non-control. Our results showed 83% area under the receiver operating characteristic (ROC) curve when OCSVM models were built using the U-Net bottleneck features of control bacteria images only. Additionally, the mean sensitivities of these one-class models are 91.67% and 86.61% for cefotaxime and piperacillin; respectively. The mean sensitivity for the prediction of ciprofloxacin is only 59.72% as the bacteria morphology was not fully detected by the proposed method.

INDEX TERMS Antibiotic resistance, *E. coli* strains, U-Net convolutional neural network, one-class SVM.

I. INTRODUCTION

Escherichia coli (*E. coli*) is a large and diverse bacterial species that can be found almost everywhere. This bacterial species shows a high degree of biological variance, where many of *E. coli* strains are essential in the digestive tract while other strains exhibit pathogenic properties and can cause many complications in the urinary tract or in the intestinal tract. On order to cure such infections, antibiotics are utilized. Their selection is becoming increasingly complicated due

The associate editor coordinating the review of this manuscript and approving it for publication was Haluk Eren.

to the overuse and misuse of these drugs yielding resistant bacteria [1]. The extensive and often unnecessary application of antibiotics both in health care as well as in agriculture increases the evolutionary pressure on these bacteria and leads to the development of new mechanisms to resist the existing antibiotics, and subsequently the antibiotics lose their ability to treat bacterial infections [2]. Consequently, the impact of antibiotic resistance is increasing dangerously to extreme levels all over the world.

To select an effective antibiotic for treating severe infections, the determination of the susceptibility profile of the causing pathogen is required. This can be achieved via antibiotic susceptibility testing (AST) which should in an ideal case be rapid, accurate and quantitative. In this context, most AST in clinical praxis relies on culturing the pathogen in the presence of antibiotics and therefore are slow, demanding an initial therapy of a patient with broad-spectrum (and sometimes ineffective) drugs, which might later be changed to a narrow spectrum antibiotic featuring the appropriate mechanism of action to cover the bacterial sensitivity profile. Traditionally, AST was performed by disk diffusion (Kirby-Bauer) methods, where the size of the growth-free zone determines the susceptibility reaction of bacterial pathogens towards a particular antibiotic [3]. Later studies recommended determining the minimal inhibitory concentration (MIC) of an antimicrobial drug. This MIC offers a precise determination of the lowest concentration (in μg/mL) of a drug that inhibits visible growth of bacteria. The classical method to identify the MIC of a specific antibiotic is still the broth micro dilution (BMD) test. Thereby, a defined volume of liquid medium is mixed with a defined concentration of the antibiotic drug and incubated for 16 to 20 h with the bacteria. Then, the MIC is read as the lowest concentration that prevents the visible bacterial growth [4]. Recently, many novel techniques for fast estimation and prediction of antibiotic susceptibility have arisen. These are mainly so-called genotypic methods including polymerase chain reaction (PCR)-based techniques [5] matrix-assisted laser desorption ionization time-of-flight mass spectrometry (MALDI-TOF MS) [6] and whole-genome sequencing [7]. Here, the existence of genes or gene products that induce resistance against certain antibiotics is detected, requiring knowledge of the resistance mechanism and the underlying gene product. Though these genotypic methods are quite fast, not all resistances will be detected, especially when they are caused by new spontaneous mutations. Innovative approaches to accelerate phenotypic AST rely on a reduced culturing period in the presence of antibiotics and a subsequent appropriate readout of phenotypic changes caused by antibiotics to susceptible bacteria. These approaches often use microfluidics [8] or microarrays [9] in addition to more sensitive detection methods like Raman spectroscopy [4], [10], [11] or real-time imaging of single cells, where in addition to the detection of the cell count, often an altered cellular morphology upon interaction with antibiotics can be detected in sensitive strains [12]. A number of morphological changes induced by antibiotics in sensitive strains have been described including -among others- filamentation, spheroplast formation, ovoid cell formation, swelling of cells and blebbing (see [13] for a review on this topic). Filamentation can be caused by several mechanisms including an inhibition of DNA synthesis, of protein synthesis and an inhibited peptidoglycan synthesis. The latter can further lead to spheroplast formation or cell lysis [13]. Each of the previously described methods for antimicrobial susceptibility detection feature its advantages and limitations regarding the type of resistance, costs and time requirements to analyze.

Nowadays, machine learning (ML) algorithms are widely implemented in several biomedical studies including the detection of the antibiotic susceptibility of bacteria. Therein, ML algorithms are designed to automate the resistance analysis for a certain AST. In this context, many applications were established to predict antimicrobial MICs [14] or to identify the bacterial resistance towards a specific antibiotic [15], [16] based on whole genome sequence (WGS) data. Also, image-based identification was often utilized to detect the morphological changes in treated bacteria using ML algorithms [12], [17], [18]. Likewise, ML approaches showed quite promising results in automating bacteria susceptibility detection based on their Raman spectra [4], [19].

In this contribution, we present an image-based approach to identify the susceptibility of *E. coli* strains with different susceptibility patterns towards the following antibiotics: ciprofloxacin, cefotaxime, piperacillin (see figure S1). Hereby, microscopic images of one *E. coli* laboratory strain and 11 clinical *E. coli* isolates were acquired, where a part was untreated and used as control bacteria while other parts were treated with different antibiotics for a short period of time (90 min). Then a combination of image processing and ML algorithms were applied to detect the morphological changes caused by these antibiotics. In our analysis, an anomaly detection approach was implemented to find the morphological changes in treated bacteria based on their images. In terms of machine learning, the task is to detect anomalous objects of a certain class, which can be performed by a one-class classifier after training it on normal objects of the same class. Using the previous property, we could train a one-class support vector machine (OCSVM) model on images of only untreated bacteria, which were utilized as control. Then image labels of treated bacteria with antibiotics were predicted as control or non-control. The detection results of *E. coli* susceptibility were presented for two types of image features and for two training methods to construct OCSVM models.

II. SAMPLE PREPARATION AND COLLECTION

Bacteria were obtained from the strain collection of the Institute of Medical Microbiology at the Jena University Hospital. AG100 is a laboratory strain derived from *E. coli* K12 and the other strains (*E. coli* 407, *E. coli* 416, *E. coli* 422, *E. coli* 455, *E. coli* 500, *E. coli* 544, *E. coli* 545, *E. coli* 554, *E. coli* 579, *E. coli* 673, *E. coli* 683) are clinical isolates from sepsis

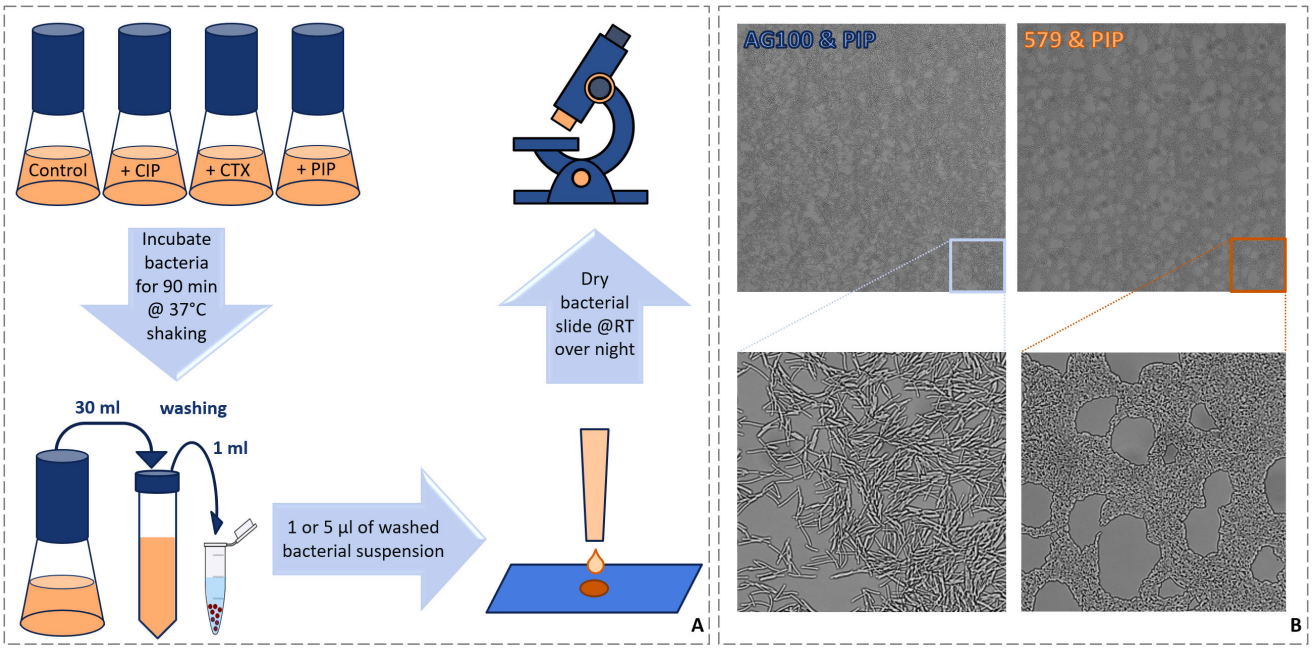

FIGURE 1. Sample preparation and image collection methods. (A) The bacteria are inoculated with three antibiotics; namely ciprofloxacin, cefotaxime and piperacillin. After inoculating, the bacteria were incubated for 90 min at 37°C, then the bacteria are washed twice in water to remove the antibiotic. Five μl of these washed bacteria are pipetted onto a slide and left to dry at room temperature (RT) over night. Finally, images of these dried bacteria are collected using a bright field microscope. (B) An example of piperacillin (PIP) interaction with *E. coli* bacteria of strains *E. coli* AG100 and *E. coli* 579. Treating bacteria of strain *E. coli* AG100 with PIP prevents bacterial growth and causes the observed morphological changes. Treating bacteria of strain *E. coli* 579 with the same antibiotic does not affect the bacterial growth.

patients at Jena University Hospital. Quantitative MIC values were determined using VITEK-2 system (bioMeìrieux) or E-Test (Liofilchem MIC Test stripes) and susceptibility categorization in sensitive (S) or resistant (R) is based on the EUCAST clinical breakpoints [20]. The upper EUCAST clinical breakpoint (R>) which categorizes resistance if the corresponding MIC is higher, was selected as test concentration (see table S1). More detailed information on the strains, their reference MIC values, and categorization are given in Kirchhoff *et al.* [4].

For each experiment, a fresh overnight culture was prepared from a −80°C bacterial cryo stock. Four culture flasks were prepared with 30 ml CASO broth (Roth GmbH); in three flasks antibiotic was added to give a final antibiotic concentration of 0.5 mg/l ciprofloxacin (ciprofloxacin hydrochloride, AppliChem), 2 mg/l cefotaxime (cefotaxime sodium, Sigma-Aldrich) or 16 mg/l piperacillin (piperacillin sodium, Sigma-Aldrich); respectively. The fourth flask served as a control without antibiotic treatment. Flasks were pre-warmed until inoculation. The overnight cultures were diluted for measuring the optical density with a spectrophotometer (Spark, Tecan) and inoculated into the pre-warmed flasks to adjust a final inoculum of 5×10^5 bacteria/ml. The cultures with and without antibiotic treatment were incubated for 90 min at 37°C while shaking at 160 rpm in an incubator (Infors HT Ecotron). After 90 min the bacterial suspensions were transferred into a tube and centrifuged for 5 min with a relative centrifugal force of 4,000 g (Universal 320R, Hettich). The bacterial pellet was re-suspended in 1 mL deionized water and washed twice by centrifuging them for 1.5 min with a relative centrifugal force of 11,500 g (MiniSpin®, Eppendorf AG). Finally, the washed pellet was suspended in 20 μl of deionized water. 1 μl and 5 μl of this suspension were pipetted onto a glass slide and allowed to dry at room temperature until the microscopic analysis. Microscopic images were acquired within 5 days after sample preparation. For each sample, a tile scan of 5×5 bright field images was recorded using an Axioobserver.Z1 (Carl Zeiss AG, Oberkochen, Germany) equipped with an LD Plan Neofluar 63x/0.75 Korr objective (Zeiss) and an Orca Flash 4.0 camera (Hamamatsu). The total imaged area per sample was 972×972 μm. On order to compensate for focal variations within the sample, 5 different focal planes with a distance of 1 μm were collected. Overall, the collected number of replicates for the strains *E. coli* 579, *E. coli* AG100 and *E. coli* 673 is four, three and two independent biological replicates; respectively, while the remaining strains were cultivated in a single biological replicate.

In this experiment, the considered centrifugation protocol is a standard technique in microbiology, and it was applied on order to concentrate the samples and wash the bacteria. These centrifugation protocols are well established and applied in numerous studies [4], [21], [22]. Nevertheless, viable bacteria have been obtained after centrifugation without any observed alteration in the bacteria behavior or in the cell morphology if

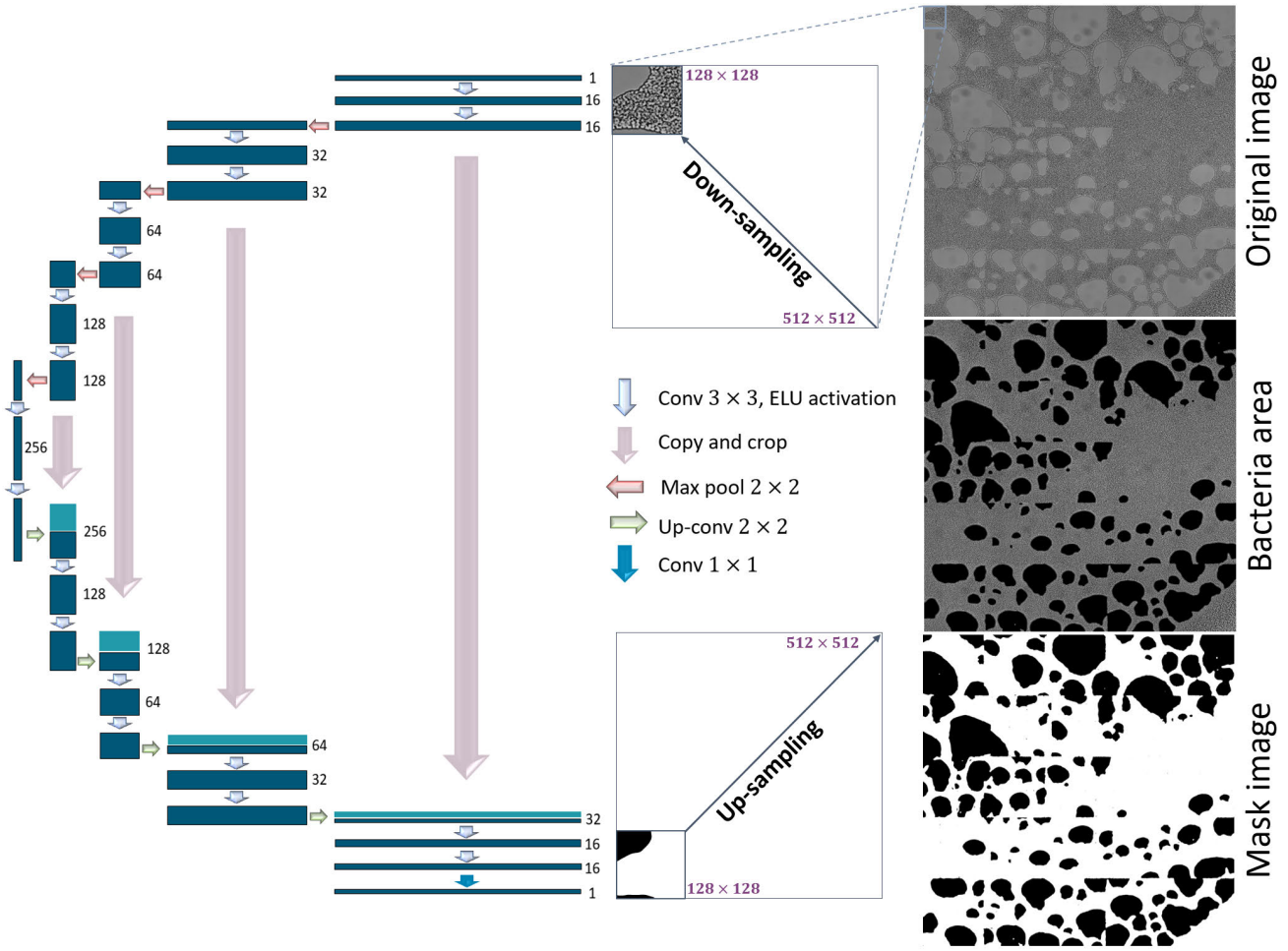

FIGURE 2. A schematic diagram of the segmentation process of the bacteria area using the U-Net network. Each bacteria image is enhanced and sliced into patches of the size 512 × 512 pixels, which are down-sampled and fed into the U-Net network. The up-sampled binary patches are stitched together to create a mask, that can be overlaid with the enhanced image on order to get the segmented image.

they were compared to samples without prior centrifugation steps (see [23]).

III. IMAGE PROCESSING AND MACHINE LEARNING

A. COMPUTATIONAL ANALYSIS

All computations were carried out based on in-house written functions in the programming language Python version 3.6.5 and the statistical programing language R version 3.4.2. The utilized packages are Scikit-learn 0.22 [24], Numpy 1.17.4 [25], OpenCV 4.1.3 [26], Pandas 0.25.3 [27], TensorFlow 2.00, Imager 0.41.2 [28] and Radiomics 0.1.3 [29]. All these functions are available upon request.

B. SEGMENTATION OF BACTERIA AREA

On order to improve the prediction of the antibiotic susceptibility and to exclude artefacts due to the drying process, only image areas with a high bacterial density were included in the analysis. Therefore, each image was segmented into a region with a high density of bacteria and a background region based on the convolutional neural network U-Net [30]. This network showed exceptional performances in semantic segmentation tasks in biomedical applications. The utilized U-Net network consists of an encoder and a decoder with four blocks in each (see Figure 2). The encoder blocks are composed of two convolutional layers, a dropout layer and a max pooling layer, while each decoder block contains an up-convolutional layer, a concatenation layer, two convolutional layers and a dropout layer. The input of the first layer of the encoder is a grayscale-image of the size 128 × 128 pixels and the output of the decoder is a binary image of the same size.

In our work, the collected bacterial images were resized into 9216 × 9216 pixels, and the image contrast was adjusted based on the contrast limited adaptive histogram equalization algorithm (CLAHE) [31]. Thereafter, the enhanced images were sliced into patches of the size 512 × × 512 pixels, and the bacterial areas of the obtained patches were predicted using the presented U-Net network. This area predication was performed for all image patches, whether they were acquired from untreated control bacteria or treated bacteria, after down-sampling the patches with a factor of four. The obtained binary patches from the U-Net were up-sampled again by

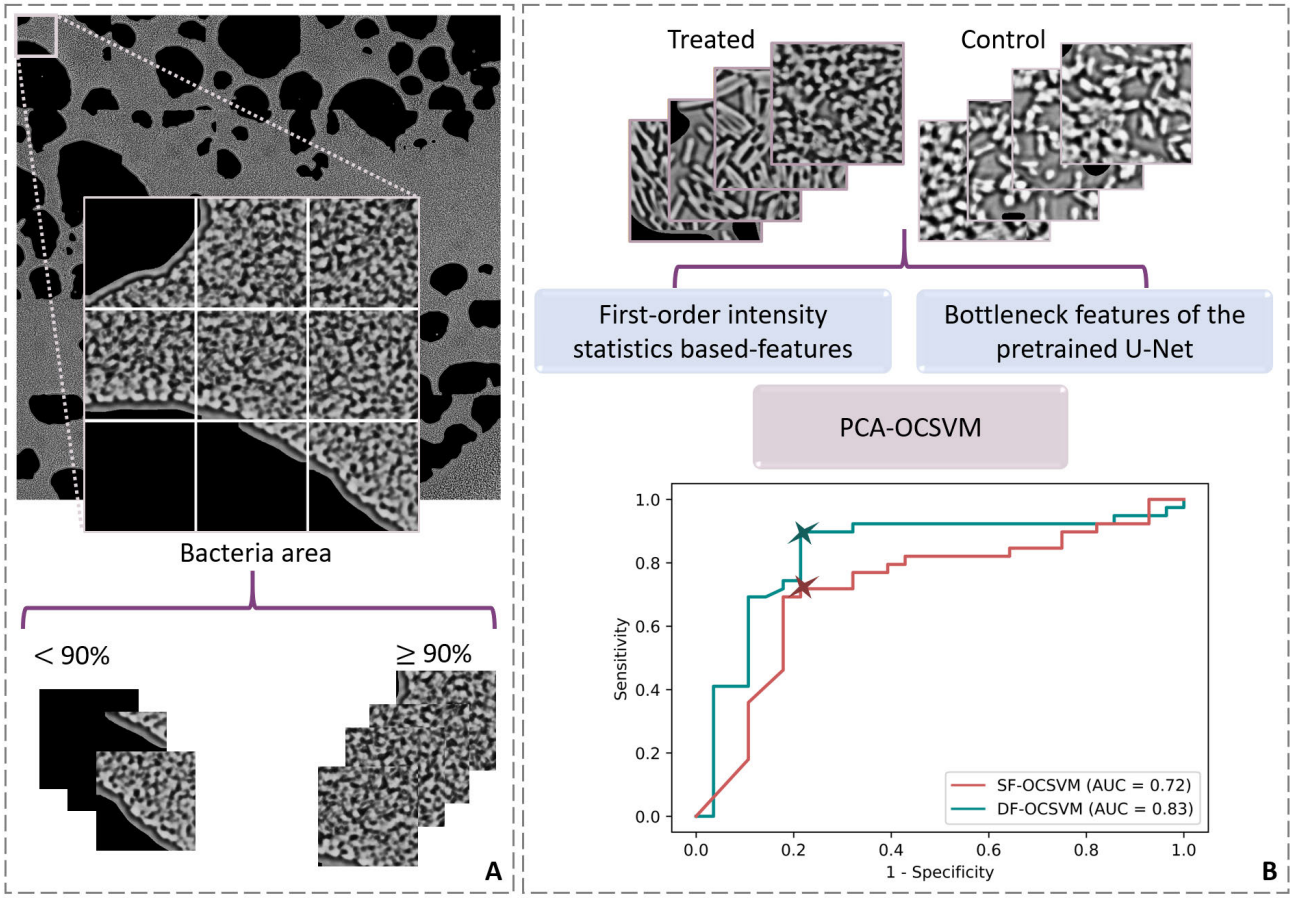

FIGURE 3. Overview of the considered patch selection method and the utilized machine learning techniques. (A) Only image patches that have 90% of their area covered by bacteria are selected to predict the antibiotic susceptibility. (B) Two types of features (SF, DF) are extracted from all selected image patches. Then the predication of the antibiotic susceptibility is performed using a once-class SVM model constructed based on features of the control patches. The obtained classifier is utilized afterwards to predict patch labels of treated bacteria.

a factor of four, and the up-sampled patches were stitched together to reconstruct a binary image with the original size of 9216×9216 pixels. This binary image separates the enhanced image into two regions; *e.g.* a bacteria containing area and a background region. Nevertheless, the training procedure of the presented U-Net network was accomplished based only on images of the strains *E. coli* AG100 and *E. coli* 579 while the bacteria area of the remaining image was not used for training the U-Net network. The selection of training set was done due to a pre-experiment, in which the antibiotic susceptibilities of stains *E. coli* AG100 and *E. coli* 579 were checked. In this per-experiment, the enhanced images of both strains were manually converted into binary images using the Java-based image processing program ImageJ [32]. Thereafter, these enhanced images and binary images were portioned with the ratio 2:1 into a training set and a validation set; respectively. Lastly, the U-Net network was trained based on the binary and the enhanced images for 50 epochs using a mini-batch of 50 patches and the Adam optimizer with a learning rate of 0.001 to minimize the binary-cross entropy loss function on the validation set. After training the U-Net, the best model was saved and utilized to segment the bacteria containing area of all remaining images. Here, the default value of learning rate for Adam optimizer was considered while the other hyperparameters; *i.e.* batch size and number of epochs, were manually selected due to the complexity of the presented segmentation task.

C. PATCH SELECTION AND FEATURE EXTRACTION

The segmented images based on the U-Net network were cut into patches of the size 256×256 pixels. Then, image patches that have at least 90% of their area covered by bacteria were selected. The previous selection of the bacteria threshold was considered to ensure approximately the same foreground areas in all selected patches (see Figure 3-A). Thereafter, the texture of the selected patches was quantified based on two types of image features. These image features are the first-order statistics-based features (SFs) of the intensity and the bottleneck features of the trained U-Net network. The latter features are indicated later as DFs. The SFs characterize texture properties of the area of interest of an image, and

they measure the spatial distribution of intensity values for image pixels [33], [34]. In our work, the energy, entropy, skewness, uniformity, kurtosis, variance, mean deviation, root mean square, mean, median, minimum and maximum were calculated for each selected patch. In table S2, the utilized statistical features were presented. Here, each feature describes a specific property of the gray level distribution of a selected patch $I(x, y)$ that has the size 256×256 pixels [34]. The other type of features; *i.e.* the DFs, can be simply extracted from the trained U-Net model after removing the decoder layers. The encoder in this case represents an image feature extractor where 256 features per patch can be extracted as it is shown in Figure 2.

D. MACHINE LEARNING FOR SUSCEPTIBILITY DETECTION

Based on the extracted features, the anomaly detection was performed to identify the susceptibility of *E. coli* strains towards the considered antibiotics. This anomaly detection is usually implemented to identify anomalous objects of a specific class [35]. The basic idea is to let a classification model learn on an available dataset in which all objects belong to a same class. Then, this learnt model is utilized to identify normal and anomalous objects of a new dataset with respect to that considered class.

For the presented study, the images of untreated control bacteria were always considered as normal objects while the treated bacterial images were predicted as normal or anomalous patches. This prediction was accomplished by comparing the intrinsic and control-specific morphology of bacterial strains with the morphological changes caused by antibiotics. So, if a particular antibiotic affects the cultivated bacteria, it changes their morphology and let these bacteria look anomalous as compared to untreated control ones (see Figure S2-A). In contrast, when the bacteria resist an antibiotic, they keep growing as untreated bacteria doing (see Figure S2-B) [36]. Under this assumption, an OCSVM model is ideal to detect the sensitivity of treated bacteria to an antibiotic drug. This detection was performed based on a principal component analysis (PCA) based dimension reduction of the feature matrix. The PCA space is formed by new uncorrelated features, i.e. the principal components, which maximize the data variance and often increase the interpretability. Then an OCSVM model was constructed using principal components (PCs) that include 99% of the variation within the untreated control bacteria patches. The obtained classifier was finally utilized to predict labels of treated bacteria as normal (control) or anomalous (non-control).

IV. RESULTS

The susceptibility identification of *E. coli* strains towards the considered antibiotics was accomplished based on a dataset comprising microscopic images collected from 12 *E. coli* strains. Within this dataset, the strains *E. coli* 579, *E. coli* AG100 and *E. coli* 673 were cultivated in four, three and two independent biological replicates; respectively, while the other *E. coli* strains were grown in a single replicate. From each replicate, images of control and treated bacteria were collected using a bright field microscope. After data acquisition, the described image processing pipeline, a patch extraction and a patch selection were applied. The selected image patches were afterwards utilized to identify the antibiotic resistance based on an OCSVM model that was trained on features extracted either from the first-order intensity statistics or from the trained U-Net network, as it is described in Figure S3.

A. THE IDENTIFICATION OF ANTIBIOTIC RESISTANCE IN E. COLI STRAINS

We present in this subsection the obtained results for predicting the antibiotic susceptibility of *E. coli* strains within each biological replicate. In Figure 3-B, a schematic view of the utilized features extraction methods and machine learning techniques is presented. For each biological replicate, the SFs and DFs were extracted, then a feature mean centering was applied with respect to the features of the control patch of each replicate. Later, two PCA models were constructed based on the extracted features from the selected untreated control patches; *i.e.* the PCA model based on the SFs and the PCA model based on DFs. Using the PCs that describes 99% of the variation within the control patch features, two OCSVM models were built. These OCSVM models represent the OCSVM based on the statistical features (SFs) named SF-OCSVM and the OCSVM based on the bottleneck features of the trained U-Net network (DFs) termed DF-OCSVM. For both models, a radial kernel was optimized for the regularization parameter $\vartheta \epsilon$ {0.001, 0.01, 0.1, 0.25, 0.50, 0.75, 0.90, 0.99} and the kernel coefficient $\gamma \epsilon$ {0.001, 0.01, 0.1, 0.25, 0.50, 0.75, 0.90, 1}. This hyperparameters optimization was accomplished via a grid search using the previous noted values of ϑ and γ. The hyperparameter values, that performed the best identification results, were selected to construct a final OCSVM model. This model was used later to predict patch labels of treated bacteria cultivated within the same replicate. As we mentioned earlier, if a specific bacterial pathogen resists an antibiotic, image patches of this pathogen are predicted as control. In contrast, if an antibiotic prevents the growth of a specific bacterial pathogen, it can change the bacteria's morphology. Therefore, the images of bacteria sensitive to this antibiotic are expected to be identified as non-control; *e.g.* dissimilar to bacteria grown without antibiotics that represent here the control bacteria. In the latest case, the untreated control and treated bacteria were cultivated in same experiment hence we are sure that any changes in the bacteria's morphology were caused only by the antibiotics. Based on these assumptions, we predicted labels for all selected patches, and we calculated the percentage of patches predicted as control for each treatment within each replicate. This percentage was denoted in the following by *CP*.

After calculating the *CP* values for bacterial images, the prediction performance of the SF-OCSVM and DF-OCSVM models was evaluated and compared using receiver operating characteristic (ROC) curves. In Figure 3-B,

the ROC curves of SF-OCSVM and DF-OCSVM models were depicted. It is clear that the OCSVM model trained on the bottleneck features of U-Net network shows larger area under the curve (AUC) than the AUC of the ROC curve obtained by SF-OCSVM models. Here, the AUC of SF-OCSVM and DF-OCSVM is 72% and 83%; respectively. In Table S1, the susceptibility predictions of bacterial image slides are presented based on two indicated thresholds of the ROC curves in Figure 3-B. These thresholds are 78.46% and 99.07%, and they are corresponding to the highest sensitivity and specificity introduced by classification models. One can note that both selected thresholds describe high values of the ROC curves, which can be interpreted that treated bacteria are predicted as control if a large percentage of image patches captured from these bacteria were classified as control patches; *i.e.* high percentages of *CP*. Nevertheless, within Table S1, antibiotic MIC values are presented beside the predictions of the *E. coli* susceptibility of both SF-OCSVM and DF-OCSVM models. Also, the antibiotic breakpoints and the reference antibiotic susceptibilities are shown with respect to each *E. coli* strain. It is observed that the OCSVM based on DFs could predict the susceptibility of *E. coli* strains toward piperacillin and cefotaxime quite well in comparison to predictions provided by the SF-OCSVM models. In contrast, neither the SF-OCSVM model nor the DF-OCSVM model could predict the susceptibility of ciprofloxacin in good manner based on the selected thresholds. In Table 1, a summary of the predicted susceptibility is presented as confusion matrices with respect to each antibiotic and each OCSVM model. For the susceptibility predictions of piperacillin, the mean sensitivity of OCSVM model increased from 41.07% to 86.61% when this classifier was trained on the bottleneck features of the U-Net network instead of using the SFs. Also, the mean sensitivity of cefotaxime improved around 4% when the DF-OCSVM was considered as the mean sensitivity of SF-OCSVM and DF-OCSVM are 87.5% and 91.67%; respectively. The mean sensitivities of SF-OCSVM and DF-OCSVM models for ciprofloxacin are only 70.14% and 59.72%. These results exhibit that the changes in bacteria morphology is not sufficient to predict the resistance towards ciprofloxacin.

TABLE 1. The confusion matrices using local OCSVM models. For each antibiotic, the reference susceptibility, and the predicted susceptibilities (S: sensitive, R: resistant) based on SF-OCSVM and DF-OCSVM models are presented, then the mean sensitivities of each antibiotic and each classifier are calculated.

Antibiotic		SF-OCSVM		M. Sens.	SD-OCSVM		M. Sens.
		R	S		R	S	
PIP	R	2	6	41.07%	7	1	86.61%
	S	3	4		1	6	
CTX	R	5	1	87.5%	5	1	91.67%
	S	1	11		0	12	
CIP	R	5	3	70.14%	6	2	59.72%
	S	2	7		5	4	

Overall, the DF-OCSVM models have better identification performance than the obtained predictions using the SF-OCSVM. These prediction results are strongly influenced by two main factors: the selected threshold by the ROC curve and the changes in bacteria shape when a particular antibiotic was applied. In case of ciprofloxacin, quite small changes in bacteria morphology were detected after incubating the bacteria while the selected threshold seems to be not suitable.

B. STUDYING THE PREDICTION PERFORMANCE OF ANTIBIOTIC SUSCEPTIBILITY BASED ON LOCAL-TRAINED/GLOBAL-TRAINED OCSVM MODEL

The main goal of the following study is to check the prediction quality of the OCSVM models based on two training techniques: the local-training and the global-training. Here, we denote by local-trained OCSVM an OCSVM model that is trained and tested on one individual replicate, while global-trained models describe the OCSVM models that are trained on a larger number of replicates and tested on other independent replicates. For local-trained models, the control bacteria images from a specific replicate are utilized to train an OCSVM model. This model is implemented to predict the resistance of treated bacteria cultivated in the same replicate but were not used for model training. A global-trained OCSVM model is built upon control images of a number of replicates, then this classifier can be utilized to predict antibiotic susceptibilities of bacteria images acquired from other replicates. In both cases, the prediction of newly acquired test data is possible and linked to the estimated accuracy. To perform such comparison, the different replicates of strain *E. coli* 579 and strain *E. coli* AG100 were considered. Therein, the bottleneck features of the trained U-Net network were extracted for all selected patches of both *E. coli* strains, and a feature mean centering was applied as was explained previously. Finally, a leave-one-replicate-out cross-validation (LORO-CV) was performed based on the PCs extracted from control patches. For model construction based on LORO-CV, we always exclude one replicate and optimize a radial kernel for the regularization parameter ϑ and the kernel coefficient γ using patches extracted from the remaining replicates. This procedure is iterated until the susceptibility of all patches selected from all replicates are identified once.

Based on the ROC curves, a comparison between the performance of local-trained OCSVM and global-trained OCSVM was performed. First of all, we calculated the *CP* values for each treatment and for all replicates. Figure 4-A presents the ROC curves of the OCSVM models using both training methods. Our results showed that the susceptibility prediction using a local-trained OCSVM model is much better than the predictions by global-trained models. Thereby, around 31% increase in the AUC can be observed by local-trained OCSVM models. In Table 2, the identification results of *E. coli* susceptibility using local-trained and global-trained models are presented based on selected thresholds of ROC curves in Figure 4-A. It turned out that a local-training for the

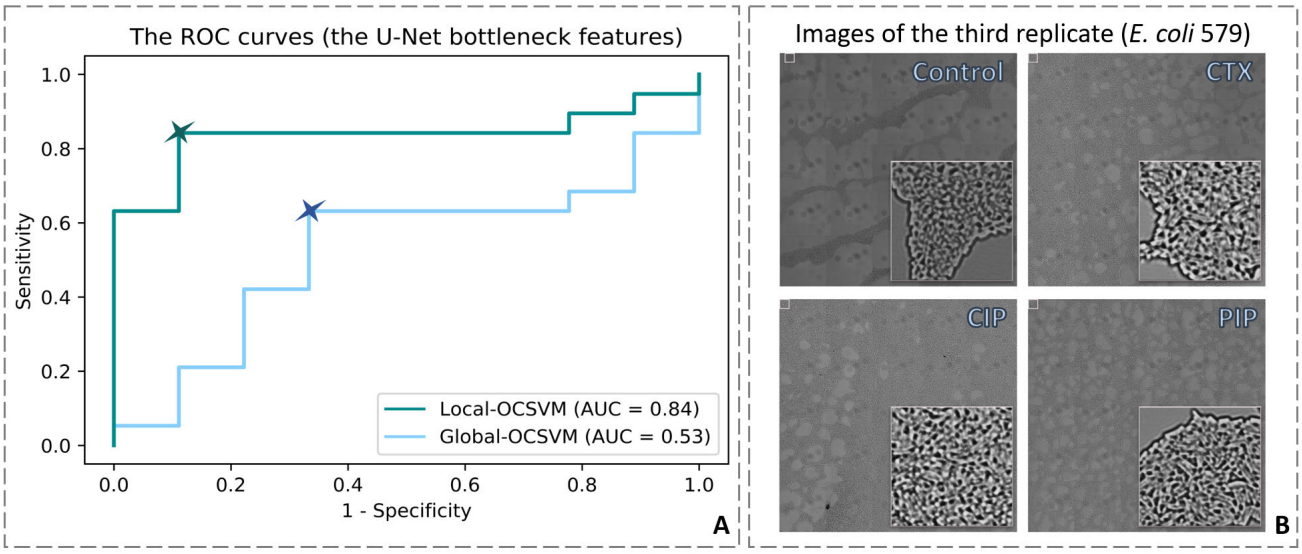

FIGURE 4. (A) The obtained ROC curves of local-OCSVM and global-OCSVM models. These models were constructed based on the bottleneck features of the trained U-Net network. The antibiotic susceptibilities were determined for the percentage of predicted patches as control (*CP*) (B) Images collected from the third replicate of strain *E. coli* 579. The reference susceptibility of *E. coli* 579 is resistant, but the image patches of the treated bacteria are obviously different to the control image patches of the strain *E. coli* 579.

TABLE 2. A comparison of local-OCSVM and global-OCSVM models. The predicted susceptibilities (S: sensitive, R: resistant) were determined based on selected thresholds. It turns out that the identification of antibiotic resistance using local-OCSVM models is much better than the predictions by global-OCSVM models.

Antibiotic & strain		Replicate	Local-OCSVM S < 80.77% & R≥ 80.77%		Global-OCSVM S < 55.20% & R ≥ 55.20%	
			CP(%)	Pred.	*CP(%)*	Pred.
Piperacillin	579 (R)	1	86.64	R	55.20	R
		2	85.76	R	65.33	R
		3	19.53	S	11.39	S
		4	80.96	R	2.57	S
	AG100 (S)	1	12.35	S	78.3	R
		2	33.39	S	45.06	S
		3	8.15	S	4.01	S
Cefotaxime	579 (R)	1	93.33	R	86.87	R
		2	88.77	R	74.22	R
		3	11.03	S	8.45	S
		4	80.77	R	0.0	S
	AG100 (S)	1	33.51	S	78.33	R
		2	29.58	S	42.72	S
		3	41.01	S	20.59	S
Ciprofloxacin	579 (R)	1	97.50	R	97.5	R
		2	90.96	R	92.4	R
		3	7.29	S	4.17	S
		4	82.82	R	0.0	S
	AG100 (S)	1	74.84	S	98.11	R
		2	85.90	R	88.83	R
		3	64.59	S	27.21	S

OCSVM models introduced a better identification of strain sensitivity compared to the identification by global-trained models. In detail, only the treated bacteria of strain *E. coli* 579 in the third replicate, and the bacteria of strain *E. coli* AG100 treated with ciprofloxacin in second replicate were misidentified when a local-trained OCSVM was considered. However, 10 images of 21 images were misclassified when a global-training for OCSVM models was applied.

The results presented above showed that the local-training of OCSVM models provide, in most cases, more stable identification results of the *E. coli* susceptibility towards antibiotics in comparison to global-trained models. These results were expected because of the high biological variations between the replicates which can confuse classifiers in case of global-trained models. Another reason for these results is that some pathogens might change their growing behavior; *e.g.* stop duplicating or interacting differently with a particular antibiotic drug. In our study, the control bacteria cultivated in the third replicate of *E. coli* 579 stopped duplicating while the treated bacteria started elongating (see Figure 4-B). Therefore, the treated patches within this replicate were mostly misclassified and were predicted as sensitive bacteria as compared to untreated control ones, even though the EUCAST clinical breakpoints indicate a resistance.

V. SUMMARY

We presented in this article the results of an image-based identification approach to detect the antibiotic susceptibilities of *E. coli* strains. The chosen antibiotics cause a strong morphological alteration in sensitive strains leading to a cell elongation (filamentation) while resistant strains retain their normal morphological properties upon treatment. In the presented work, different image processing techniques were combined with machine learning algorithms on order to automate the susceptibility detection. We started the analysis by enhancing the image contrast, and we segmented the high-bacterial density areas based on the U-Net network. The segmented images were afterwards cut into patches, and the patches that have at least 90% of their area covered

by bacteria were selected for further analyses composed of feature extraction and modeling. In our work, the first-order statistics-based features of the intensity (SFs) and the bottleneck features of the trained U-Net network (DFs) were extracted and used to train a one-class classification model; specifically, an OCSVM model. This type of classification is designed to detect anomalous objects of a particular class after training the model only on normal objects of this considered class.

Based on the described data analysis pipeline, we performed two comparisons to identify the *E. coli* susceptibility using OCSVM models. In the first comparison, the antibiotic sensitivity of each bacterial replicate was predicted using a local-OCSVM model that was built on both types of image features. The second comparison was performed to check the prediction quality of the OCSVM models using two training methods and using the DFs only. The results of the first comparison showed that using the DFs to train local-OCSVM models introduced larger area under the ROC curve than the SF-OCSVM models. Also, for selected thresholds of ROCs, the classification mean sensitivities of piperacillin and cefotaxime increased from 41.07% to 86.61% and from 87.5% to 91.67%; respectively, when OCSVM models were constructed on the bottleneck features instead of using the SFs. In contrast, both classifiers showed low identification results based on the selected thresholds when the bacterial pathogens were treated by ciprofloxacin. To investigate this behavior, the DFs were utilized to perform the second comparison. Therein, two training techniques; namely local-training and global-training, were compared. While a local-OCSVM model was trained and tested on untreated control and treated bacteria patches of the same replicate, different independent replicates were utilized to train and test the global-OCSVM models. The evaluation of these models proved that locally trained one-class models feature a great potential in identifying the antibiotic sensitivity as compared to global-trained OCSVM models.

VI. CONCLUSION

It was shown that the combination of bottleneck features of the trained U-Net and the local trained OCSVM models introduced quite promising results in identifying the susceptibility of *E. coli* strains towards antibiotics. These local models are correcting for the biological variations between different replicates or patients and yielding better predictions of individual patient's susceptibility towards antibiotics. Therefore, the presented local-one-class classification approach can be easily implemented to predict other antibiotic susceptibilities, and an easy image-based antibiotic susceptibility tests (ASTs) can be generated. Since the morphological changes appear already after short incubation times of antibiotics with bacteria (90 min), this image-based method might be used for the development of fast phenotypic AST, maybe in combination with statistical parameters from other readout methods like Raman spectroscopy.

ACKNOWLEDGMENT

Support information: Figure S1, S2, S3 and Table S1, S2.

REFERENCES

[1] (2020). *Antibiotic Resistance*. [Online]. Available: https://www.who.int/topics/antimicrobial_resistance/en/

[2] C. L. Ventola, "The antibiotic resistance crisis: Part 1: Causes and threats. P & T : A peer-reviewed," *J. Formulary Manage.*, vol. 40, no. 4, pp. 277–283, 2015.

[3] C. Giuliano, "A guide to bacterial culture identification and results interpretation. P & T : A Peer-Reviewed," *J. Formulary Manage.*, vol. 44, no. 4, pp. 192–200, 2019.

[4] J. Kirchhoff, U. Glaser, J. A. Bohnert, M. W. Pletz, J. Popp, and U. Neugebauer, "Simple ciprofloxacin resistance test and determination of minimal inhibitory concentration within 2 h using Raman spectroscopy," *Anal. Chem.*, vol. 90, no. 3, pp. 1811–1818, Feb. 2018.

[5] M. R. Pulido, "Progress on the development of rapid methods for antimicrobial susceptibility testing," *J. Antimicrob Chemother*, vol. 68, no. 12, p. 2710, 2013.

[6] V. Belkum, "Matrix-assisted laser desorption ionization time-of-flight mass spectrometry in clinical microbiology: What are the current issues," *Ann. Lab. Med.*, vol. 37, no. 6, pp. 475–483, 2017.

[7] M. J. Ellington, "The role of whole genome sequencing in antimicrobial susceptibility testing of bacteria: Report from the EUCAST subcommittee," *Clin. Microbiol. Infection*, vol. 23, no. 1, pp. 2–22, Jan. 2017.

[8] J. Campbell, C. McBeth, M. Kalashnikov, A. K. Boardman, A. Sharon, and A. F. Sauer-Budge, "Microfluidic advances in phenotypic antibiotic susceptibility testing," *Biomed. Microdevices*, vol. 18, no. 6, p. 103, Dec. 2016.

[9] A. Srinivasan, G. C. Lee, N. S. Torres, K. Hernandez, S. D. Dallas, J. Lopez-Ribot, C. R. Frei, and A. K. Ramasubramanian, "High-throughput microarray for antimicrobial susceptibility testing," *Biotechnol. Rep.*, vol. 16, pp. 44–47, Dec. 2017.

[10] K. Chang, "Antibiotic susceptibility test with surface-enhanced Raman scattering in a microfluidic system," *Anal. Chem.*, vol. 91, no. 17, pp. 10988–10995, 2019.

[11] A. Tannert, R. Grohs, J. Popp, and U. Neugebauer, "Phenotypic antibiotic susceptibility testing of pathogenic bacteria using photonic readout methods: Recent achievements and impact," *Appl. Microbiol. Biotechnol.*, vol. 103, no. 2, pp. 549–566, Jan. 2019.

[12] J. Choi, J. Yoo, M. Lee, E.-G. Kim, J. S. Lee, S. Lee, S. Joo, S. H. Song, E.-C. Kim, J. C. Lee, H. C. Kim, Y.-G. Jung, and S. Kwon, "A rapid antimicrobial susceptibility test based on single-cell morphological analysis," *Sci. Transl. Med.*, vol. 6, no. 267, pp. 174–267, Dec. 2014.

[13] T. P. T. Cushnie, N. H. O'Driscoll, and A. J. Lamb, "Morphological and ultrastructural changes in bacterial cells as an indicator of antibacterial mechanism of action," *Cellular Mol. Life Sci.*, vol. 73, no. 23, pp. 4471–4492, Dec. 2016.

[14] M. Nguyen, "Using machine learning to predict antimicrobial MICs and associated genomic features for nontyphoidal salmonella," *J. Clin. Microbiol.*, vol. 67, no. 2, 2019, Art. no. e01260.

[15] E. S. Kavvas, E. Catoiu, N. Mih, J. T. Yurkovich, Y. Seif, N. Dillon, D. Heckmann, A. Anand, L. Yang, V. Nizet, J. M. Monk, and B. O. Palsson, "Machine learning and structural analysis of mycobacterium tuberculosis pan-genome identifies genetic signatures of antibiotic resistance," *Nature Commun.*, vol. 9, no. 1, p. 4306, Dec. 2018.

[16] M. W. Pesesky, T. Hussain, M. Wallace, S. Patel, S. Andleeb, C.-A.-D. Burnham, and G. Dantas, "Evaluation of machine learning and rules-based approaches for predicting antimicrobial resistance profiles in gram-negative bacilli from whole genome sequence data," *Frontiers Microbiol.*, vol. 7, p, 5, Nov. 2016.

[17] M. Marschal, "Evaluation of the accelerate pheno system for fast identification and antimicrobial susceptibility testing from positive blood cultures in bloodstream infections caused by gram-negative pathogens," *J. Clin. Microbiol.*, vol. 55, no. 7, p. 2116, 2017.

[18] H. Yu, W. Jing, R. Iriya, Y. Yang, K. Syal, M. Mo, T. E. Grys, S. E. Haydel, S. Wang, and N. Tao, "Phenotypic antimicrobial susceptibility testing with deep learning video microscopy," *Anal. Chem.*, vol. 90, no. 10, pp. 6314–6322, May 2018.

[19] C.-S. Ho, N. Jean, C. A. Hogan, L. Blackmon, S. S. Jeffrey, M. Holodniy, N. Banaei, A. A. E. Saleh, S. Ermon, and J. Dionne, "Rapid identification of pathogenic bacteria using Raman spectroscopy and deep learning," *Nature Commun.*, vol. 10, no. 1, p. 4927, Dec. 2019.

[20] D. Kusic, "Raman spectroscopic characterization of packaged L. Pneumophila strains expelled by T. Thermophila," *Anal. Chem.*, vol. 88, no. 5, pp. 2533–2537, 2016.
[21] U. Schröder, "On-chip spectroscopic assessment of microbial susceptibility to antibiotics within 3.5 hours," *J. Biophoton.*, vol. 10, no. 11, pp. 1547–1557, 2017.
[22] T. Ursell, T. K. Lee, D. Shiomi, H. Shi, C. Tropini, R. D. Monds, A. Colavin, G. Billings, I. Bhaya-Grossman, M. Broxton, B. E. Huang, H. Niki, and K. C. Huang, "Rapid, precise quantification of bacterial cellular dimensions across a genomic-scale knockout library," *BMC Biol.*, vol. 15, no. 1, p. 17, Dec. 2017.
[23] J. Choi, H. Y. Jeong, G. Y. Lee, S. Han, S. Han, B. Jin, T. Lim, S. Kim, D. Y. Kim, H. C. Kim, E.-C. Kim, S. H. Song, T. S. Kim, and S. Kwon, "Direct, rapid antimicrobial susceptibility test from positive blood cultures based on microscopic imaging analysis," *Sci. Rep.*, vol. 7, no. 1, Dec. 2017, Art. no. 1148.
[24] F. Pedregosa, "Scikit-learn: Machine Learning in Python," *J. Mach. Learn. Res.*, vol. 1, pp. 2825–2830, Nov. 2011.
[25] T. E. Oliphant, *A Guide to NumPy*, vol. 1. New York, NY, USA: Trelgol Publishing, 2006.
[26] G. Bradski, "The OpenCV library," *Dr. Dobb's J. Softw. Tools*, 2000.
[27] W. McKinney, "Data structures for statistical computing in Python," in *Proc. 9th Python Sci. Conf.*, 2010, pp. 1–5.
[28] S. Barthelmé and D. Tschumperlé, "Imager: An r package for image processing based on CImg," *J. Open Source Softw.*, vol. 4, no. 38, p. 1012, Jun. 2019.
[29] J. Carlson, "Radiomics: 'Radiomic' image processing toolbox," *R Package Version 0.1*, vol. 2, 2016.
[30] O. Ronneberger and P. T. F. Brox, *U-Net: Convolutional Networks for Biomedical Image Segmentation*. Cham, Switzerland: Springer, 2015.
[31] A. Reza, "Realization of the contrast limited adaptive histogram equalization (CLAHE) for real-time image enhancement," *J. VLSI Signal Process. Syst. Signal, Image Video Technol.*, vol. 38, no. 1, pp. 35–44, 2004.
[32] J. Schindelin, "Fiji: An open-source platform for biological-image analysis," *Nat. Methods*, vol. 9, no. 7, pp. 676–682, 2012.
[33] R. M. Haralick and K. I. Shanmugam Dinstein, "Textural features for image classification," *IEEE Trans. Syst., Man, Cybern.*, vol. SMC-3, no. 6, pp. 610–621, Nov. 1973.
[34] C. Parmar, E. Rios Velazquez, R. Leijenaar, M. Jermoumi, S. Carvalho, R. H. Mak, S. Mitra, B. U. Shankar, R. Kikinis, B. Haibe-Kains, P. Lambin, and H. J. W. L. Aerts, "Robust radiomics feature quantification using semiautomatic volumetric segmentation," *PLoS ONE*, vol. 9, no. 7, Jul. 2014, Art. no. e102107.
[35] V. Hodge and J. Austin, "A survey of outlier detection methodologies," *Artif. Intell. Rev.*, vol. 22, no. 2, pp. 85–126, Oct. 2004.
[36] J. L. Martínez and F. Baquero, "Interactions among strategies associated with bacterial infection: Pathogenicity, epidemicity, and antibiotic resistance," *Clin. Microbiol. Rev.*, vol. 15, no. 4, p. 647, 2002.

NAIRVEEN ALI received the B.Sc. and M.Sc. degrees in mathematical statistics from Damascus University, in 2009 and 2014, respectively. She is currently pursuing the Ph.D. degree with the Research Group of Statistical Modeling and Image Analysis, University of Jena, supervised by PD. Dr. Bocklitz. Her research interests include multivariate data analysis, image processing, and machine learning for biomedical applications.

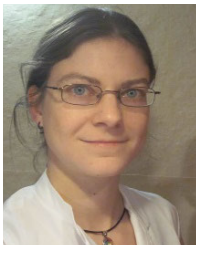

JOHANNA KIRCHHOFF received the Diploma degree in biology and the Ph.D. degree in physical chemistry from Friedrich Schiller University Jena, in 2012 and 2019, respectively. In 2014, she started her Ph.D. research in the group of Prof. Neugebauer with the Center for Sepsis Control and Care (CSCC) and the Leibniz Institute of Photonic Technology (IPHT), Jena. Her Ph.D. project was focused on micro-Raman spectroscopic characterization of the interactions of antibiotics with sepsis pathogens. Her research interests include new optical-spectroscopic procedures for microbiological diagnosis and antimicrobial susceptibility testing strategies.

PATRICK IGOCHE ONOJA received the B.Sc. degree in physics from Benue State University, Nigeria, in 2006, and the M.Sc. degree in biomedical engineering from Heidelberg University, Germany, in 2014. He is currently pursuing the second M.Sc. degree in the research group of Dr. Popp and under the supervision of PD. Dr. Christoph Krafft. From 2015 to 2016, he worked as a Student Research Assistant in the group of Dr. G. Glatting with the Mannheim University Hospital. In 2018, he joined with Dr. Ute Neugebauer, where he studied microscopic characterization of antibiotic bacteria interaction. His research interests include radiation therapy, biomedical imaging, spectroscopy, and microscopy of biological samples.

ASTRID TANNERT received the degree in biochemistry from Martin-Luther-University Halle-Wittenberg, the University of Wales, Cardiff University, and the Free University of Berlin, and the Ph.D. degree in biophysics from the Humboldt University of Berlin, in 2003. She is currently coordinating the Jena Biophotonic and Imaging Laboratory. Her research interest includes microscopic solutions for biomedical research and diagnosis especially in infectious diseases.

UTE NEUGEBAUER studied chemistry in Jena, Germany, and Chapel Hill, NC, USA. After her Ph.D. degree, she joined the Biomedical Diagnostics Institute, Dublin, Ireland. From 2011 to 2016, she was leading the Junior Research Group Spectroscopic Pathogen Detection at the Center for Sepsis Control and Care (CSCC), Jena University Hospital. Since 2016, she has been a Professor with the University of Jena, the Department Leader with the Leibniz Institute of Photonic Technology, Jena, and the Head of the Core Unit Biophotonics, CSCC. Her research interests include novel spectroscopic tools and methods for medical diagnostics and the characterization of physiological interactions with a special focus on infection and sepsis.

JÜRGEN POPP received the degree in chemistry from the Universities of Erlangen and Würzburg, the Ph.D. degree in chemistry, and the Habilitation degree from the University of Würzburg, in 2002. After his Ph.D. degree in chemistry, he joined Yale University for his postdoctoral studies. Since then, he has held a Chair of physical chemistry with Friedrich Schiller University Jena. He has also been the Scientific Director of the Leibniz Institute of Photonic Technology, Jena, since 2006. His research interest includes biophotonics, in particular with the development and application of innovative Raman techniques for biomedical diagnosis.

THOMAS BOCKLITZ received the Diploma degree in theoretical physics, in 2007, the Ph.D. degree in chemometrics, in 2011, and the degree in physics and mathematics from Friedrich Schiller University Jena. He is currently the Junior Research Group Leader of statistical modeling and image analysis with the University of Jena. His research interest includes the translation of physical information, obtained by AFM, TERS, Raman spectroscopy, CARS, SHG, or TPEF, into medically or biologically relevant information.